chemosensors

MDPI

Article

A "Turn-Off" Pyrene-Based Ligand as a Fluorescent Sensor for the Detection of Cu^{2+} and Fe^{2+} Ions: Synthesis and Application in Real Water Samples, Logic Gate Construction, and Bio-Imaging

Bhavana G. Gowda [1], Muzaffar Iqbal [2] and Shiva Prasad Kollur [1,*]

[1] School of Physical Sciences, Amrita Vishwa Vidyapeetham, Mysuru Campus, Mysuru 570 026, Karnataka, India
[2] Department of Pharmaceutical Chemistry, College of Pharmacy, King Saud University, Riyadh 11451, Saudi Arabia; muziqbal@ksu.edu.sa
* Correspondence: shivachemist@gmail.com

Abstract: Herein, we report the synthesis and characterization of a novel Schiff base ligand, (Z)-5-((pyren-1-ylmethylene)amino)-2,4-dihydro-3H-pyrazol-3-one (**PMDP**). The characterization of ligand **PMDP** was carried out using ESI-MS, ^{1}H NMR, and UV–Visible spectroscopic techniques. As a probe, **PMDP** displayed a detectable, colorimetric colour shift in the presence of Cu^{2+} and Fe^{2+} ions. The solution was seen to have a light brown colour and to exhibit a fluorometric "turn off" response when Cu^{2+} and Fe^{2+} ions were present in a DMSO solution (HEPES 0.01 M, pH = 7.4) at room temperature. Job's plot revealed that the **PMDP** binding ratio to Cu^{2+} and Fe^{2+} ions was in 1:2 ratio. In contrast to the other metal ions (Cd^{2+}, Mn^{2+}, Co^{2+}, Na^{+}, Ni^{2+}, Cu^{+}, Fe^{3+}, Hg^{2+}, Mg^{2+}, Zn^{2+}, K^{+}, and V^{5+}), the synthesised probe showed exceptional sensitivity and selectivity for detecting Cu^{2+} and Fe^{2+} metal ions. The results indicate that the detection limits for Cu^{2+} and Fe^{2+} are 0.42 μM and 0.51 μM, respectively. Furthermore, **PMDP** was efficiently utilised for the quantitative analysis of Cu^{2+} and Fe^{2+} in real water samples, RGB colour values in smart phones, logic gate construction, and cell imaging in HeLa cells.

Keywords: fluorescent sensor; Schiff base; real water sample; cell imaging

Citation: Gowda, B.G.; Iqbal, M.; Kollur, S.P. A "Turn-Off" Pyrene-Based Ligand as a Fluorescent Sensor for the Detection of Cu^{2+} and Fe^{2+} Ions: Synthesis and Application in Real Water Samples, Logic Gate Construction, and Bio-Imaging. *Chemosensors* **2024**, *12*, 91. https://doi.org/10.3390/chemosensors12060091

Received: 29 April 2024
Revised: 20 May 2024
Accepted: 28 May 2024
Published: 30 May 2024

1. Introduction

In recent years, scientists working in the field of chemical sensors have focused on the development and synthesis of novel nitrogen-containing heterocyclic Schiff-base compounds. Likewise, they have concentrated on employing these compounds as fluorescent and colorimetric chemosensors for the identification and detection of species that are important to the environment and biology, such as metal cations and anions. Transition metal ions have a wide range of possible uses in biology, medicine, catalysis, and environmental applications. Building a highly sensitive and selective chemosensor is therefore essential for the identification of transition metals. The trace elements Fe^{2+} and Cu^{2+} are the most important of all the transition metal ions [1–4].

Copper ranks as the third most prevalent metal ion in the biological system. Copper is involved in many biological processes in the human body, such as the synthesis of haemoglobin, the body's utilisation of iron, immune system function, bone health, and changes in cholesterol metabolism [5–7]. Copper is also a catalytic co-factor for metalloenzymes. Cu^{2+} contributes to environmental degradation since it is widely used in numerous sectors. The maximum content of Cu^{2+} in drinking water, as per the drinking water standards set by the World Health Organization is 2 parts per million (~30 micrograms per million) [8,9]. Heart disease, foregut surgery, nutritional deficiencies, enteropathies

with malabsorption, and prolonged intravenous nutrition (total parenteral nutrition) can all result from a copper deficit in humans. Excessive amounts can lead to Menke's and Alzheimer's illness, and Wilson's disease, and toxic levels of copper that induce nausea, vomiting, diarrhoea, and nose irritation. Copper must be detected using colorimetric and fluorometric techniques in biological and environmental systems due to these negative effects [10]. On the other hand, iron, the second most common metal after aluminium, makes up around 5% of the earth's crust. It is crucial for the transfer of oxygen by haemoglobin, cellular metabolism, enzyme catalysis, and a few enzymatic processes. On the other hand, an excess of iron in the body can lead to several serious illnesses. Anaemia, diabetes, heart disease, liver and kidney damage are all brought on by a Fe^{2+} deficit. Hemochromatosis and gastrointestinal system damage can result from the body absorbing too much Fe^{2+} [11,12]. Therefore, creating sensors that can identify Fe^{2+} is crucial, even though it is currently believed to be difficult.

Because of the importance of these two metal ions in biology, medicine, and environmental systems, research into developing chemosensors to detect Cu^{2+} and Fe^{2+} ions has been considered particularly valuable. Traditionally, a wide range of spectroscopic techniques for identifying these metal ions are documented in the literature [12], including voltammetry, atomic absorption spectrometry (AAS), and inductively coupled plasma atomic emission spectrometry (ICPAES). Among these techniques, colorimetric "naked-eye" chemosensors and fluorescence have been used extensively for metal ion detection because of their ease of use, simplicity, low detection limit, high sensitivity, and low selectivity. Furthermore, single probes for several targets have been thoroughly investigated because of benefits like possible cost savings and faster processing times [13–15].

In order to detect various analytes, we synthesised a chemosensor in this work for the reasons described above. Furthermore, this probe has the ability to concurrently detect the two metal ions that are most prevalent and important in the environment, Cu^{2+} and Fe^{2+}, using two different sensing techniques (colorimetric responses and fluorescence responses).

2. Materials and Methods

All solvents and reagents were used as received from commercial sources without any further purification. The compounds 1-Pyrene carboxaldehyde, 3-Amino-1H-pyrazol-5(4H)-one, and all metal (II) chloride and nitrites salts of Cd^{2+}, Cu^{2+}, Fe^{3+}, Mn^{2+}, Co^{2+}, Na^{+}, Ni^{2+}, Cu^{+}, Fe^{3+}, Hg^{2+}, Zn^{2+}, K^{+}, Mg^{2+}, and V^{5+} were procured from Avra synthesis (Bengaluru, India). All reactions were performed on oven-dried glass ware. A Bruker Avance NMR instrument was used to record ^{1}H spectra at 400 MHz, respectively. The PL spectra were recorded with a Shimadzu RF-6000 spectro-fluorophotometer (Tokyo, Japan). A Shimadzu UV-3101 spectrophotometer was used to record the UV–vis spectra of the solutions.

2.1. Synthesis of Ligand (PMDP)

The general reaction represented in Scheme 1 illustrates the steps involved in the synthesis of the Schiff base ligand. First, 10 mL of a hot ethanolic solution was used to dissolve 57 mg (0.25 mM) of 1-pyrenecarboxaldehyde. To this solution, 2–3 drops of H_2SO_4 were added, which worked as a catalyst during the chemical reaction. Adding 24 mg (0.25 mM) of 3-Amino-1H-pyrazol-5(4H)-one to this clear solution resulted in an immediate colour change from yellow to brown. The reaction mixture was continuously stirred at room temperature for 12 h. The resulting brown precipitate was filtered and washed with ethanol to obtain the final pure product.

Yield: 76%; m.p.: 183 °C; ^{1}H-NMR (DMSO-d_6; 400 MHz, ppm): δ—9.18 (s, 1H), 7.88–6.23 (m, 9H), 2.95 (s, 2H) (Figure S1) ^{13}C-NMR (DMSO-d_6; 100 MHz, ppm): δ—172.43, 162.20, 149.90, 149.19, 138.69, 137.85, 135.99, 128.99, 128.83, 128.78, 128.46, 127.34, 123.59, 122.17 (Figure S2); Mass (*m/z*): Calcd. 311.12 [M^{+}], Expt. 312.17 [M + 1] (Figure S3). FT-IR (KBr pallet): 1615 cm^{-1} (azomethine group), 1587 cm^{-1} (carbonyl stretching) (Figure S6).

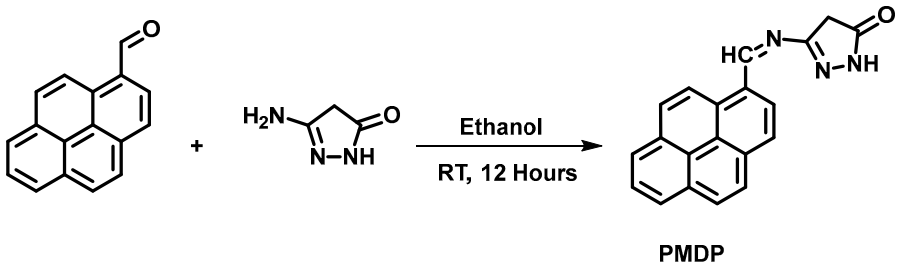

Scheme 1. General synthetic route for obtaining Schiff base ligand **PMDP**.

2.2. Synthesis of Metal Complexes

An ethanolic solution of metal ions [$FeSO_4 \cdot 7H_2O$ and $CuCl_2 \cdot 2H_2O$] was added dropwise to an ethanolic solution of **PMDP** in a 1:2 (metal–ligand) molar ratio. Further, the mixture was continuously stirred at 60 °C for 2 h. The product thus obtained was dried and purified through recrystallisation in hot ethanol, dried, and used for further analysis.

PMDP-Cu^{2+} complex: Yield: 61%; Mass (*m*/*z*): Calcd. 686.46 [M^+], Expt. 687.94 [M + 1] (Figure S4).

PMDP-Fe^{2+} complex: Yield: 63%; Mass (*m*/*z*): Calcd. 676.73 [M^+], Expt. 677.87 [M + 1] (Figure S5).

2.3. Cytotoxicity Assay and Cell Imaging

The cytotoxic impact of the **PMDP** ligand on cells was determined using the MTT (5-dimethylthiazol-2-yl-2,5-diphenyltetrazolium bromide) assay [16]. To achieve approximately 75% confluence before the treatment, HeLa cells were plated on a 36-well plate and cultured for a full day. The cells in the 36-well plate were then cultured for an additional 24 h after the addition of **PMDP** (0–100 µL). The cells were then grown for four hours after MTT (5 mg/mL; 50 µL/well) was added to each well. After adding 200 µL of DMSO to each well, the absorbance at 316 nm was determined.

Dulbecco's Modified Eagle Medium (DMEM) was used to cultivate HeLa cells at 37 °C in an environment containing 5% CO_2. After 30 min, **PMDP** staining was performed, and the cells were cleaned using PBS buffer solution. With the aid of an Invitrogen EVOS M5000 fluorescent inverted microscope (Washington, WA, USA), fluorescence cell imaging was accomplished.

3. Results and Discussions

3.1. UV–Visible Titration Studies

The primary method of investigating the UV–Vis absorption studies of the probe **PMDP** towards different metal ions, such as Cd^{2+}, Cu^{2+}, Fe^{2+}, Mn^{2+}, Co^{2+}, Na^+, Ni^{2+}, Hg^{2+}, Zn^{2+}, K^+, V^{5+}, Mg^{2+}, Cu^+, and Fe^{3+}, was to monitor them in DMSO solution with 60 µM (HEPES, 10 mM pH 7.4) at room temperature. First, we examined the probe's colorimetric properties with and without metal ions. The probe **PMDP** functions as a chemosensor for Cu^{2+} and Fe^{2+} upon the addition of one equivalent of each type of metal ion (confirmed using mass spectral results, as depicted in Figures S3 and S4). The $\pi \rightarrow \pi^*$ transition of the C=N group was represented by discrete absorption peaks in the UV–Vis titration of **PMDP** at 333 nm, and the $n \rightarrow \pi^*$ transition resulting from intramolecular charge transfer (ICT) involving donor–acceptor conjugation systems was reflected at 350 nm [17,18]. The absorption peaks at 333 and 350 nm were first blueshifted to 313 and 330 nm for Cu^{2+} and 301 and 330 nm for Fe^{2+}, respectively, after being treated with these metal ions (Figure 1). The solution's hue transitioned from bright yellow to light brown (Figure 2). This demonstrates how **PMDP** forms a compound by coordinating with Cu^{2+} and Fe^{2+} ions, respectively. According to the above-described experiment, Cu^{2+} and Fe^{2+} ions can be colorimetrically determined via a "naked-eye" analysis of **PMDP** in the DMSO solution.

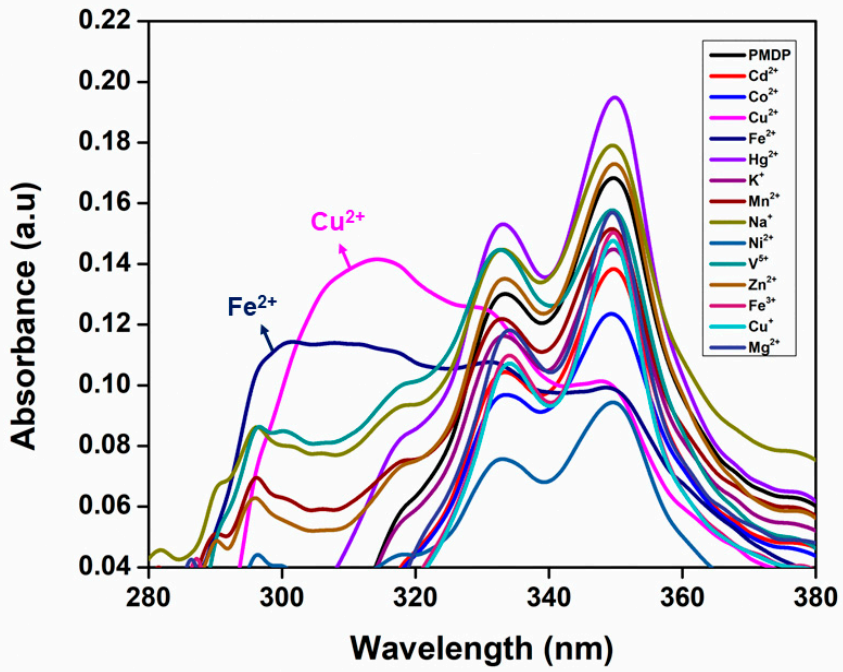

Figure 1. UV–Visible absorbance spectrum of **PMDP** (60 μM, HEPES 0.01 M, pH = 7.4) in DMSO solution at room temperature with different metal ions (40 μM).

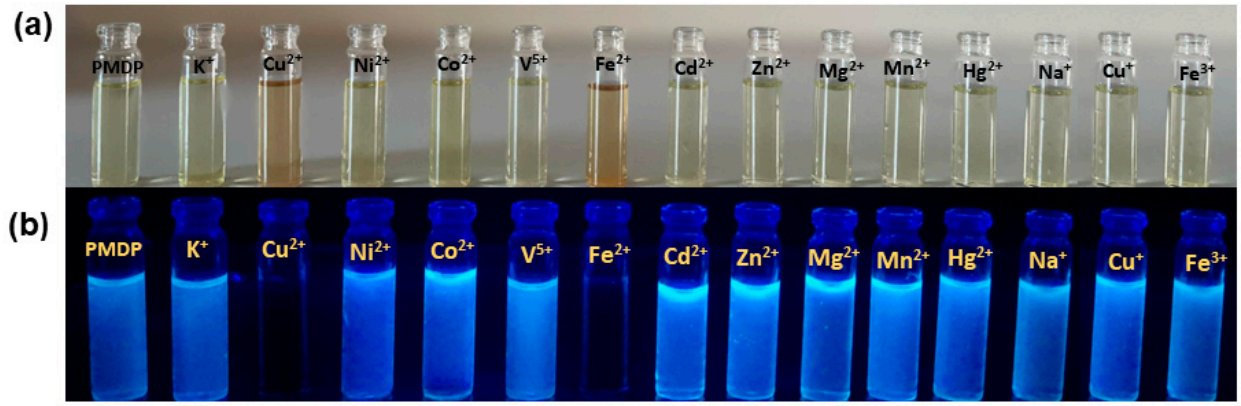

Figure 2. Images demonstrating how the addition of various metal ions (40 μM) altered the fluorescence of **PMDP** (60 μM, DMSO, HEPES 0.01 M, pH = 7.4) under (**a**) white light (**b**) UV light.

3.2. Fluorescence Studies

In order to evaluate **PMDP**'s selectivity towards different metal ions such as Cd^{2+}, Cu^{2+}, Fe^{2+}, Mn^{2+}, Co^{2+}, Na^{+}, Ni^{2+}, Cu^{+}, Fe^{3+}, Hg^{2+}, Zn^{2+}, K^{+}, V^{5+}, and Mg^{2+} in a DMSO solution in the presence of 60 μM (HEPES, 0.01 M pH 7.4) at room temperature, fluorescence emission tests were carried out (Figure 3). After being excited at 350 nm, the ligand's fluorescence spectra showed an emission band spanning from 370 to 430 nm. Fluorescence enhancement is caused by the addition of the metal ions Cd^{2+}, Mn^{2+}, Co^{2+}, Na^{+}, Ni^{2+}, Hg^{2+}, Zn^{2+}, K, Mg^{2+}, and V^{5+} to the ligand. Due to the formation of a complex between **PMDP** and the Cu^{2+} and Fe^{2+} metal ions, there was a significant effect on decreasing the emission intensity of the fluorescence spectra; the fluorescence spectra of the ligand only slightly change for the other metal ions. Because of this, the sensor shows a noticeable turn-off of fluorescence when Cu^{2+} and Fe^{2+} are present. The interaction between Cu^{2+} and Fe^{2+} ions and the probe results in a notable quenching of fluorescence intensity [19]. For the purpose of selectively detecting Cu^{2+} and Fe^{2+} ions, respectively, the chemosensor functions as an excellent selective fluorescence on–off sensor probe.

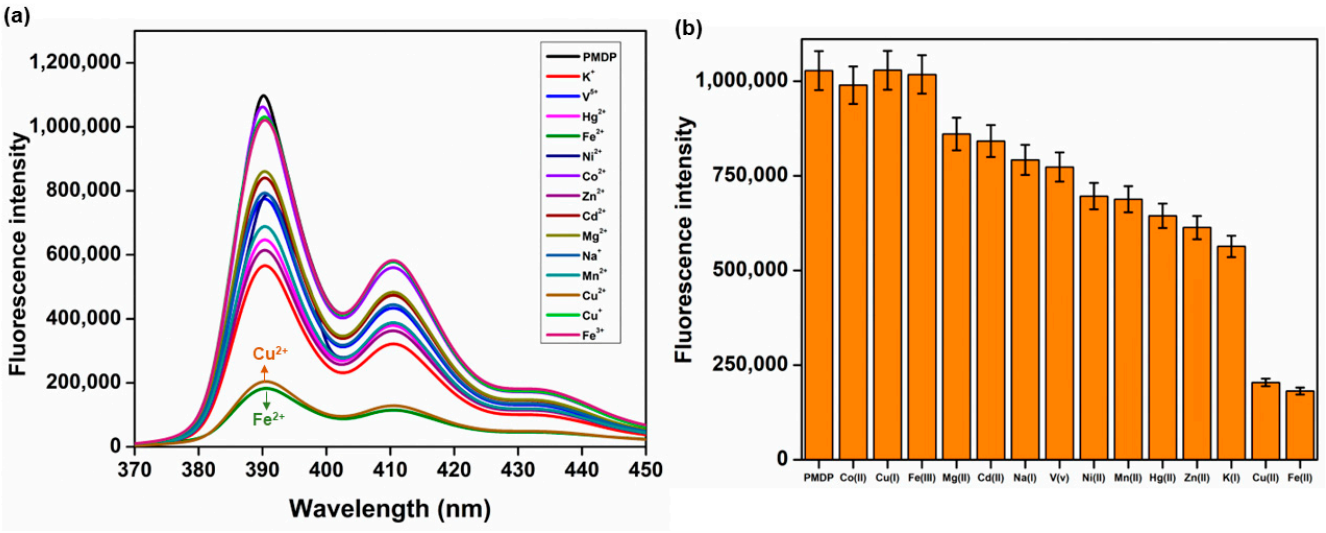

Figure 3. (**a**) Fluorescence intensity spectra of **PMDP** (60 μM) in DMSO solution (HEPES 0.01 M, pH = 7.4) in presence of various metal ions (40 μM) upon excitation at 350 nm (**b**) The change in fluorescence intensity of **PMDP** (60 μM) in DMSO solution (HEPES 0.01 M, pH = 7.4) in the presence of different metal ions (40 μM) upon excitation at 350 nm.

3.3. Competitive Studies

In order to determine the degree of validity and selectivity of **PMDP** (60 μM) for the detection of Cu^{2+} and Fe^{2+} ions in a DMSO solution, competitive metal ions, namely Cd^{2+}, Mn^{2+}, Co^{2+}, Na^{+}, Ni^{2+}, Cu^{+}, Fe^{3+}, Hg^{2+}, Zn^{2+}, K^{+}, V^{5+} and Mg^{2+} ions, were competitively titrated. Each of these metal ions exhibited a noticeable increase in fluorescence at λ_{ex} 350 nm. The ligand **PMDP's** fluorescence intensity was quenched in the presence of other metal ions upon the addition of Cu^{2+} and Fe^{2+}, indicating some interference. When **PMDP** interacts with competitive metal ions in a 1:1:1 ratio (L:M^{2+}:Cu^{2+}/Fe^{2+}), interference is seen. All metal ions appear to have investigated the turn-off mechanism as a result of the influence of the metal ions Cu^{2+} and Fe^{2+}. PMDPs selectivity for Cu^{2+} and Fe^{2+} ions is strongly demonstrated by the results shown in the bar intensity graph, even in the presence of competing metal ions, as shown in Figure 4.

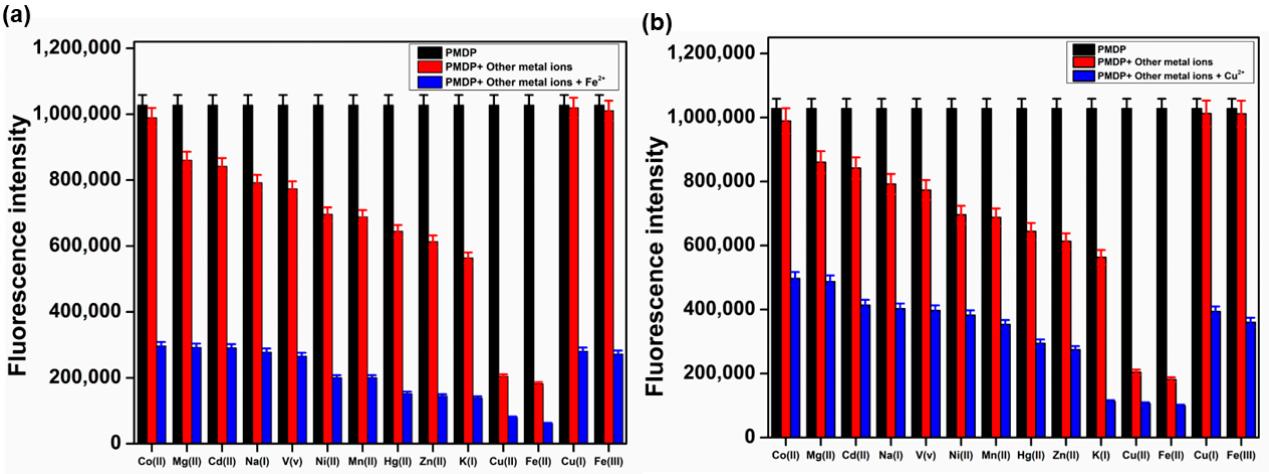

Figure 4. Fluorescence intensity spectrum of **PMDP** (60 μM) in DMSO solution (HEPES 0.01 M, pH = 7.4) in the presence of various competitive metal ions (40 μM) with (**a**) Fe^{2+} and (**b**) Cu^{2+} (40 μM) upon excitation at 350 nm.

3.4. Job's Plot

Using Job's titration approach, the stoichiometry of the **PMDP** ligand with the Cu^{2+} and Fe^{2+} metal complex was determined [20]. By plotting the absorbance vs. mole fraction of the Cu^{2+} and Fe^{2+} complex at 350 nm, the stoichiometry of the metal complex between the ligand and metal ions was ascertained. A number of solutions containing **PMDP** (30 mM) and Cu^{2+} and Fe^{2+} (30 mM) were prepared (10 mL) in order to guarantee that the volume remained constant. Furthermore, the maximal electronic absorption intensity for both metal ions at a ratio of 0.3 M suggested a 1:2 stoichiometric binding relationship between the **PMDP** and the Cu^{2+} and Fe^{2+} ions (Figure 5).

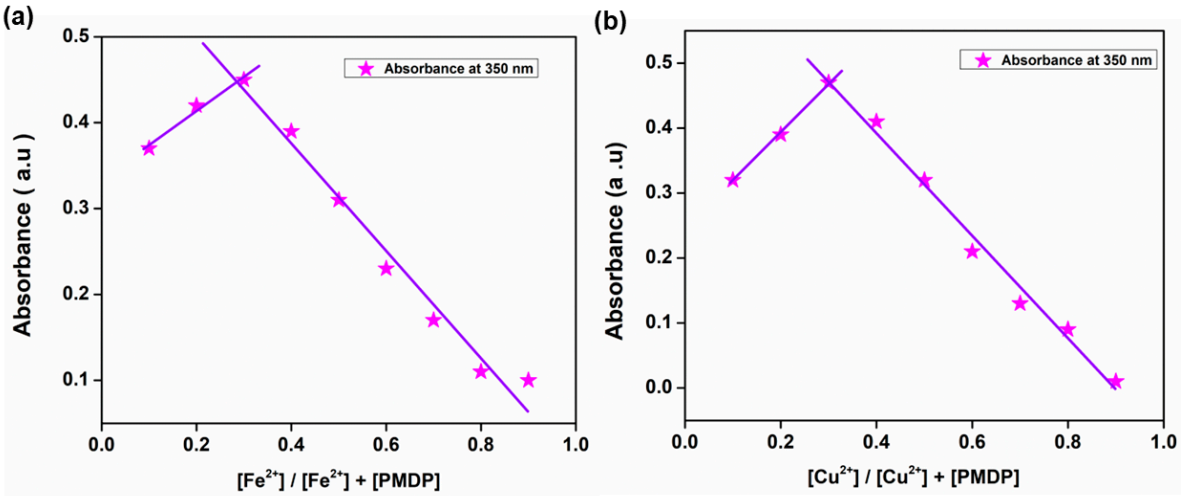

Figure 5. Job's plot for determining stoichiometry of **PMDP** in DMSO solution (60 μM, 0.01 M HEPES, pH = 7.4), in presence of 40 μM of (**a**) Cu^{2+} and (**b**) Fe^{2+} ions.

3.5. Solvent Effect

The probe **PMDP**'s response to the Cu^{2+} and Fe^{2+} ions was further investigated at the maximal emission intensity in a range of solvents, including DMSO, DMF, acetonitrile, methanol, ethanol, and THF. It was discovered that the type of solvent used affects the fluorescence intensity that the chemosensor can display. As shown in Figure 6, **PMDP** only displayed its maximal fluorescence intensity to the greatest extent in the DMSO solution.

3.6. Stern–Volmer Analysis

The sensitivity of the **PMDP** sensor to Cu^{2+} and Fe^{2+} ions was determined by fluorescence titration with solutions at concentrations ranging from 0 to 100 μM. Adding up to 100 μM of Cu^{2+} and Fe^{2+} ions to the chemosensor solution resulted in the effective quenching of fluorescence intensity, with maximum emissions at occurring at 390 nm at 350 nm excitation wavelengths (Figure 7). The chemosensor's fluorescence intensity gradually decreased as the concentrations of Cu^{2+} and Fe^{2+} ions increased. The interaction between the Cu^{2+} and Fe^{2+} ions and the probe **PMDP** resulted in a notable reduction in fluorescence intensity. In a Stern–Volmer analysis, this fluorescence titration approach was utilised to evaluate the ligand-quenching process with metal ions (Cu^{2+} and Fe^{2+}). When the detecting metal ions were added, the fluorescence intensity steadily decreased. The association constant was determined using the modified Stern–Volmer Equation (1) [21].

$$F_0/F = K_{sv}\,[Q] + 1 \quad (1)$$

where F_0 and F represent the ligand's fluorescence intensity in the absence and presence of varying metal ion concentrations. The Stern–Volmer constant is denoted by K_{sv}, and the overall concentrations of Cu^{2+}/Fe^{2+} ions are represented by [Q]. Graphs were plotted

against F_0/F values with various concentrations of Cu^{2+} and Fe^{2+} metal ions, revealing that the K_{sv} of the samples was 6.9×10^5 M^{-1} for Fe^{2+} and 7.3×10^5 M^{-1} for Cu^{2+}.

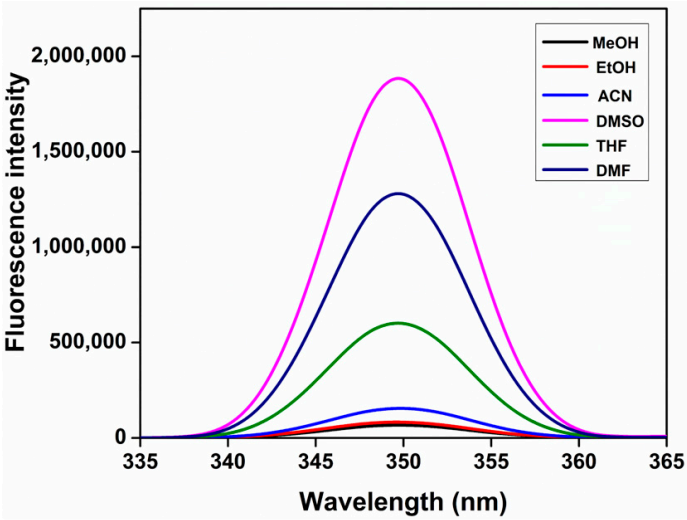

Figure 6. Fluorescence intensity spectrum of **PMDP** (60 μM) with various solvents.

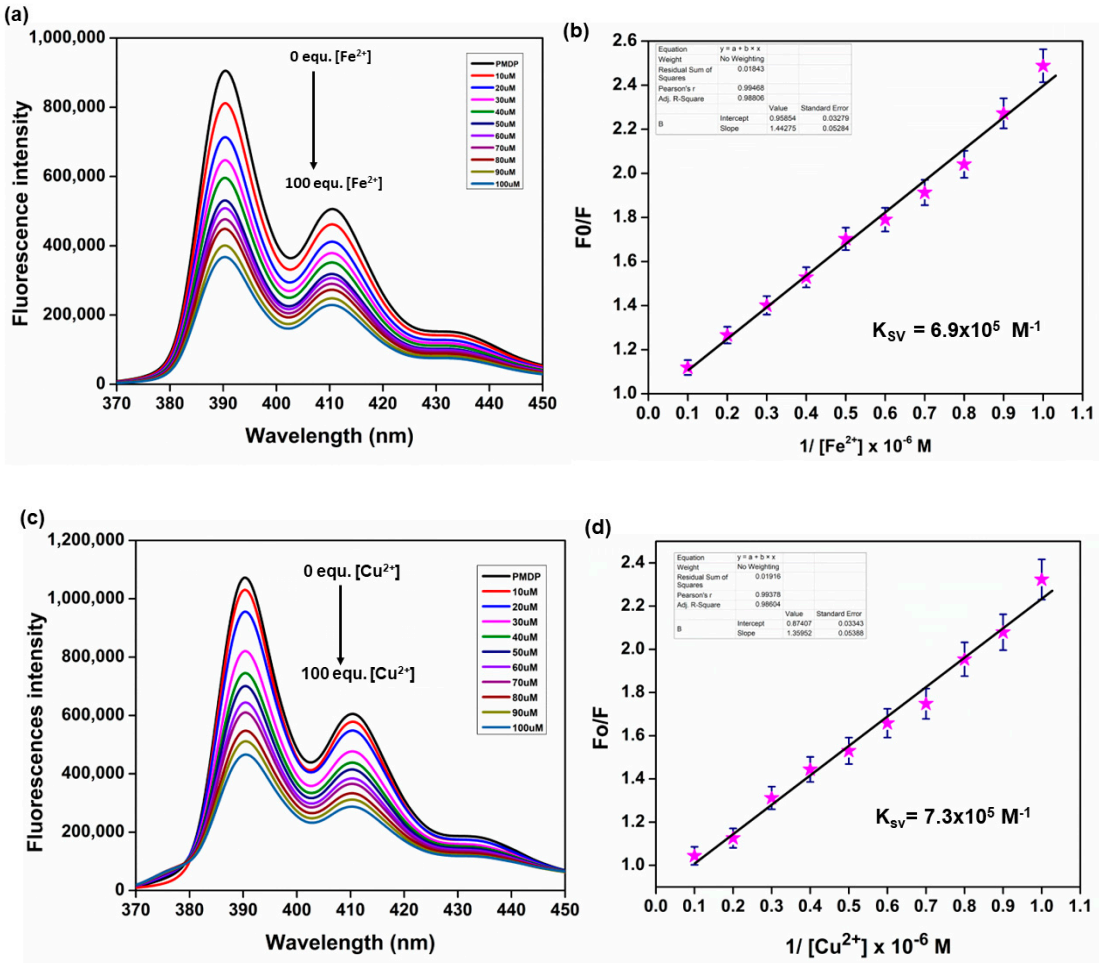

Figure 7. Fluorescence emission spectra of **PMDP** upon addition of (**a**) Fe^{2+} and (**c**) Cu^{2+} ions (0–100 equivalents) in DMSO (60 μM, 0.01 M HEPES, pH = 7.4) at excitation 350 nm. Linear graph of fluorescence intensity versus inverse concentration of (**b**) Fe^{2+} and (**d**) Cu^{2+} at 350 nm upon gradual addition of metal ions.

3.7. Reversible Nature of PMDP

Reversibility determines whether a probe can be repeatedly detected, which is a crucial factor in practical applications. It must have an excellent reversible property in order to be a good metal sensor. Binding Cu^{2+} and Fe^{2+} ions with the probe **PMDP** produced fluorescence in the reversibility experiment [22]. As such, we supplemented the solutions **PMDP**-Cu^{2+} and **PMDP**-Fe^{2+} with the chelating ligand EDTA as a standard metal-complexing agent. As depicted in Figure 8, upon the addition of EDTA, the fluorescence spectra of **PMDP**-Cu^{2+} and **PMDP**-Fe^{2+} were identical to that of the **PMDP** without the inclusion of Cu^{2+} and Fe^{2+} ions. In addition, adding Cu^{2+} and Fe^{2+} ions to the **PMDP** + Cu^{2+} + EDTA and **PMDP** + Fe^{2+} + EDTA mixes causes the fluorescence intensity to gradually drop once more. The results of the reversible cycle suggest that the probe **PMDP** can be detected repeatedly; therefore it could be reused at least five times by adding an EDTA solution and a metal ion solution as replacements (Figure 9). Based on the results, **PMDP**'s reversible cycle performance greatly increased its potential for use in logic gate design.

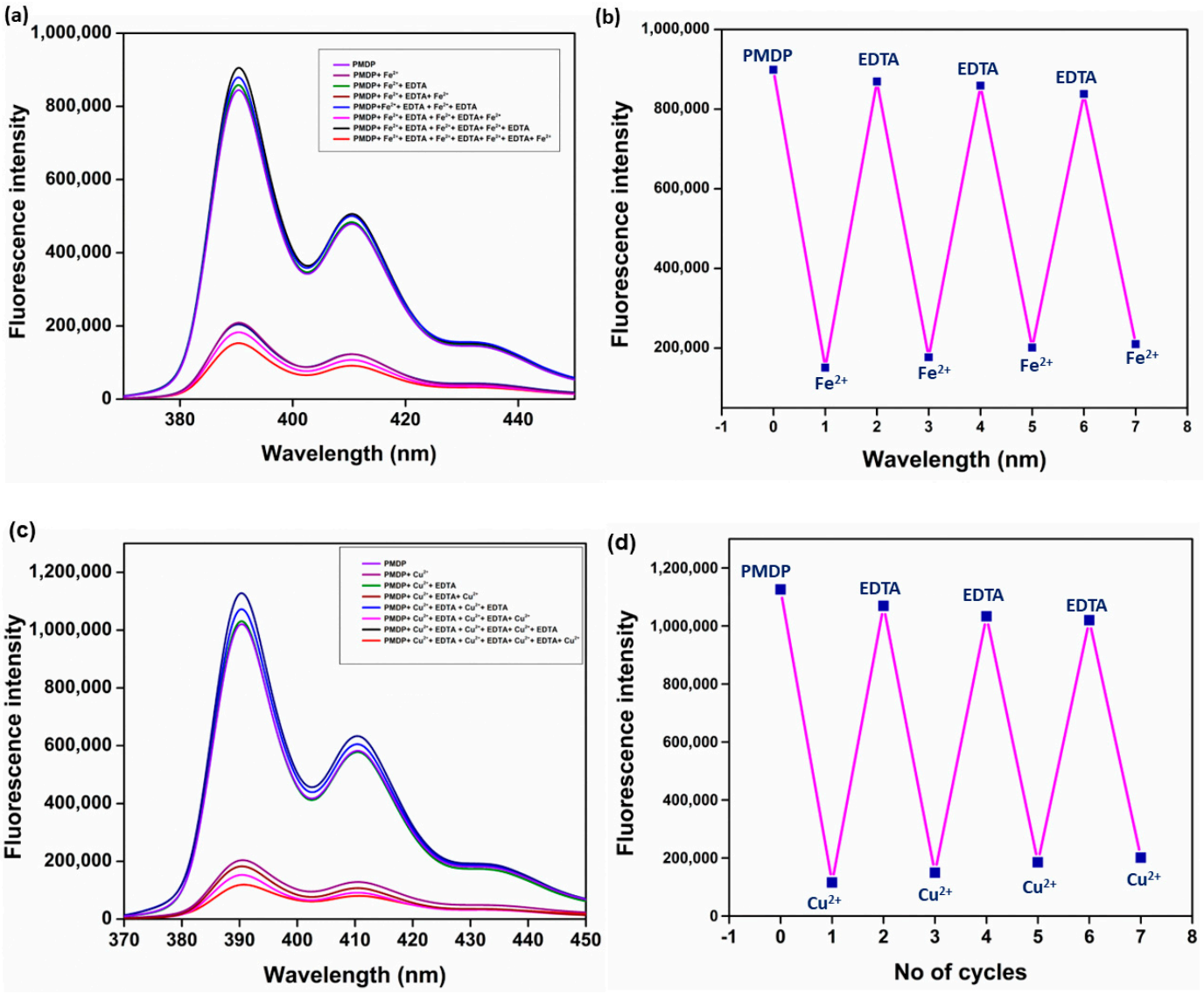

Figure 8. Fluorescence emission spectrum of reversible sensing nature of **PMDP** with (**a**) Fe^{2+} and (**c**) Cu^{2+} and EDTA. Reversibility cycle occurs following alternate addition of (**b**) Fe^{2+} and (**d**) Cu^{2+} and EDTA in DMSO (60 μM, 0.01 M HEPES, pH = 7.4) upon excitation at 350 nm.

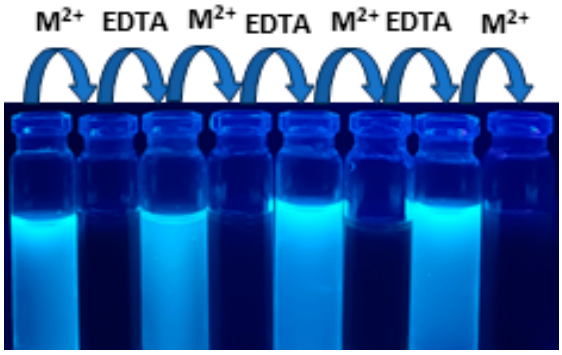

Figure 9. Colour changes in the ligand **PMDP** when M^{2+} (Cu^{2+}/Fe^{2+}) and EDTA were added alternately while exposed to UV light.

Furthermore, the chelation rate (R) of EDTA in a reversible EDTA experiment was determined by fluorescence emission studies. Initially the reaction was as zero-order reaction calculated using Equation (2), where the rate of the reaction is equal to rate constant. From Figure 10, it clear that the rate constant is the slope of the linear graph [23]. The calculated rate constants (k) for Fe^{2+} and Cu^{2+} are 2.9 × 10^3 Ms^{-1} and 3.8 × 10^3 Ms^{-1}. The chelation rate, which expresses the rate at which the reactant is being consumed or the product is being produced, is directly proportional to the rate constant *k* in a zero-order reaction [24,25].

$$\text{Rate} = -\frac{d[A]}{dt} = k[A]^0 = k = \text{constant} \quad (2)$$

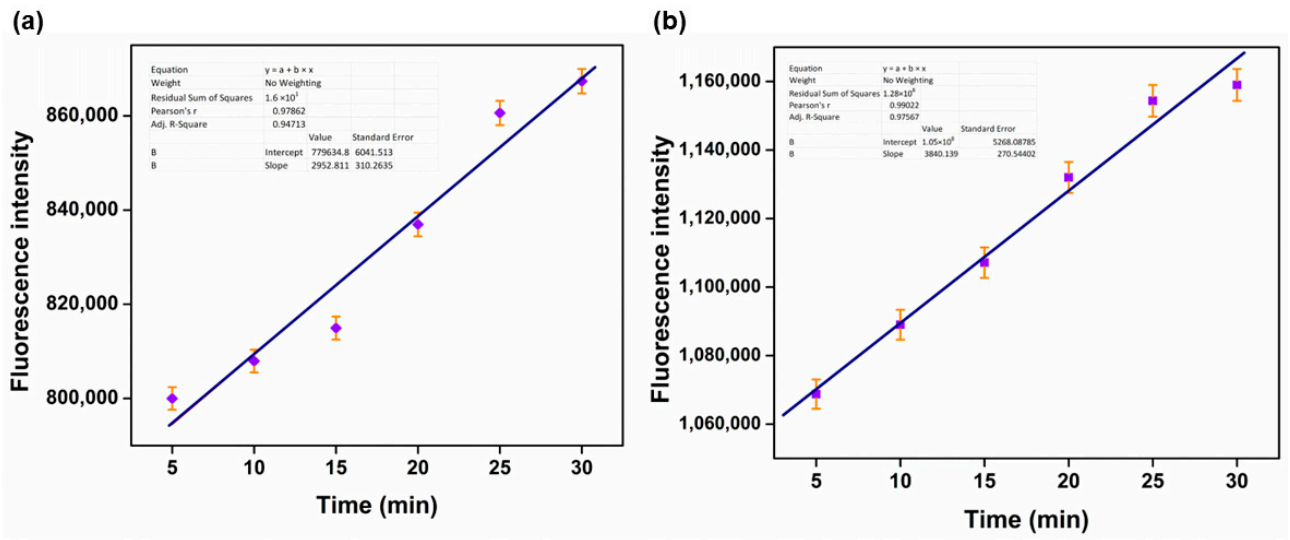

Figure 10. Chelation rate determination using a linear graph. The graph is plotted between the fluorescence intensity versus time of (**a**) Fe^{2+} and (**b**) Cu^{2+} at 390 nm upon excitation at 350 nm.

3.8. pH Effect

A pH of 1–14 was achieved by adding HCl or NaOH to 10 mM of Bis-Tris buffer. Each pH buffer was placed into a cuvette following the addition of 60 µL of **PMDP**. the absorption spectra of **PMDP** in each of the different pH buffers was measured using a UV–Vis spectrophotometer. Each solution was then mixed with 3 µL of Fe^{2+} and Cu^{2+} ions, respectively. The complex's absorption response at different pH values was noted. Figure 11 indicates that the behaviour of **PMDP**'s and the complex's absorption at 350 nm was consistent throughout the different pH values. Even under extremely basic and acidic conditions, there was very little change in the absorption spectra that could be seen due to

pH variations. The aforementioned findings indicate that the sensors may find extensive use in several physiological and environmental contexts [26].

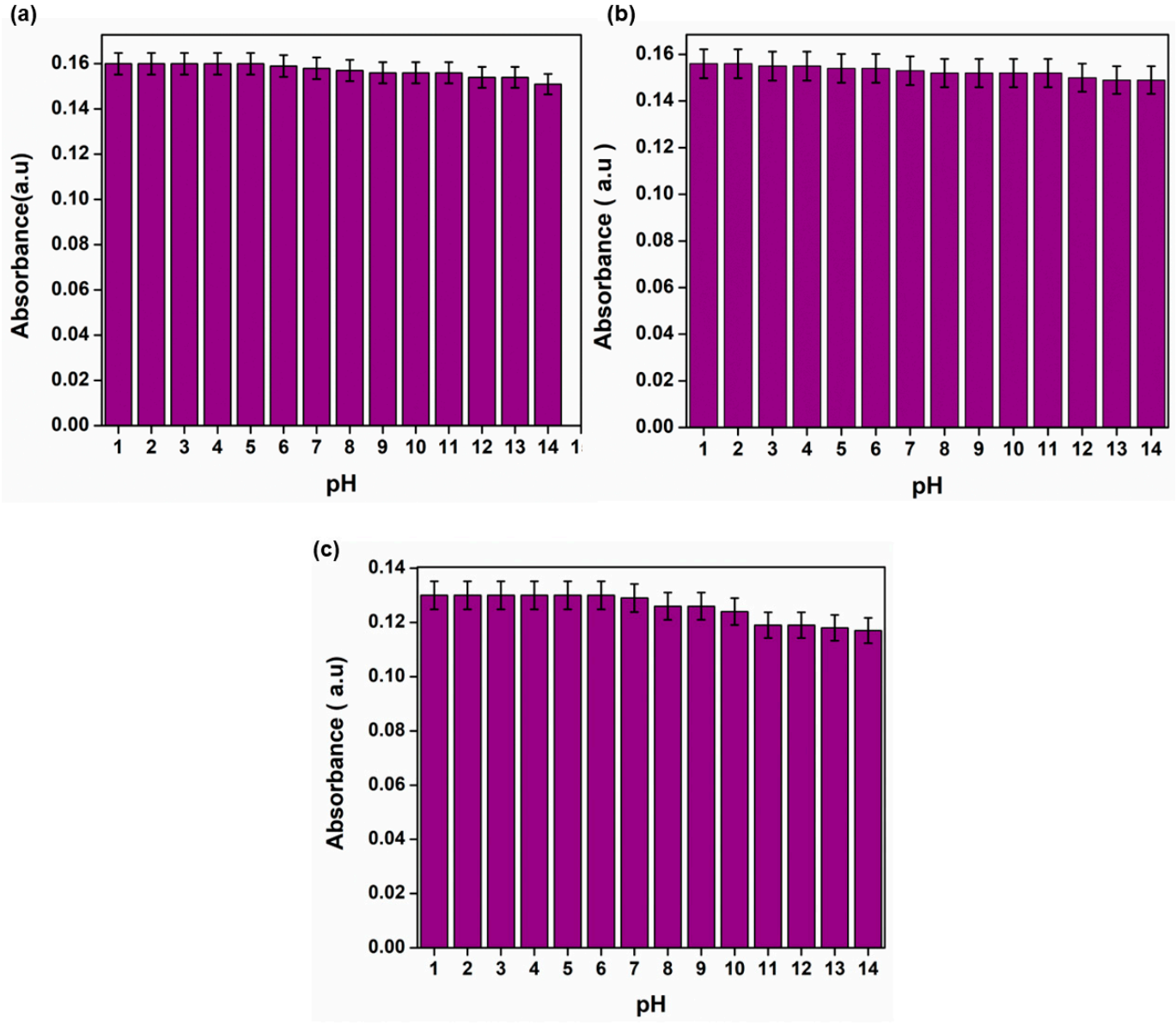

Figure 11. Absorbance of (**a**) **PMDP**, (**b**) **PMDP** + Fe^{2+}, and (**c**) **PMDP** + Cu^{2+} under different pH conditions at 350 nm.

3.9. Limit of Detection (LOD) Investigation

The limit of detection (LOD) of **PMDP** was calculated by changing the concentrations of Cu^{2+} and Fe^{2+} ions while keeping the **PMDP** concentration constant. The absorption spectra were produced using 50 µL of **PMDP** in DMSO, showing that the absorbance rises linearly with increasing Cu^{2+} and Fe^{2+} ion concentrations. For the Cu^{2+} and Fe^{2+} ions, the **PMDP** detection limit was computed using the following formula [27,28]:

$$\text{Detection limit} = 3.3\ \sigma/k$$

where σ represents the standard deviation of the response curve and k represents the slope of the calibration curve. The limit of detection was determined to be 0.42 µM and 0.51 µM for Cu^{2+} and Fe^{2+} by plotting the absorbance graph against the concentrations of Cu^{2+} and Fe^{2+} ions, as is shown in Figure 12.

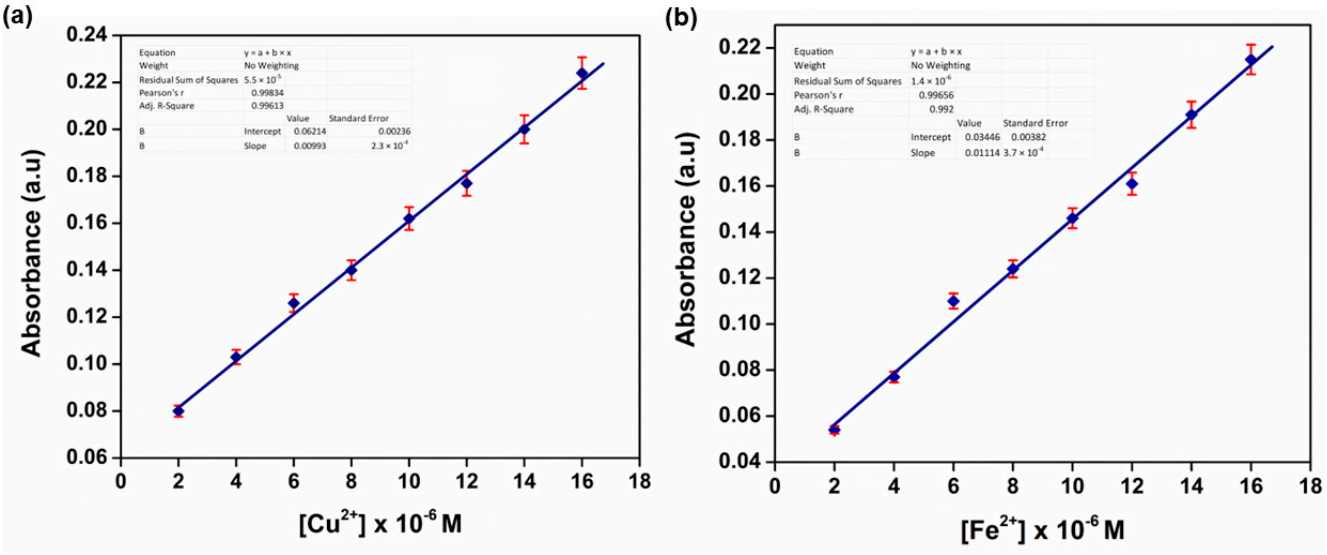

Figure 12. Absorption of calibration curve of **PMDP** in DMSO solution (60 μM, HEPES 0.01 M, pH 7.4) upon adding different concentrations of (**a**) Cu^{2+} solution and (**b**) Fe^{2+} solution.

3.10. Kinetic Data Determaination

The kinetic data of the probe's reaction with Cu^{2+} and Fe^{2+} ions were determined by plotting a graph of the fluorescence intensity versus time. As depicted in Figure 13, the rate constant k was derived from the slope of the above linear graph. The calculated rate constants for Fe^{2+} and Cu^{2+} were 3.95 × 10^2 Ms^{-1} and 2.4 × 10^2 Ms^{-1}, respectively.

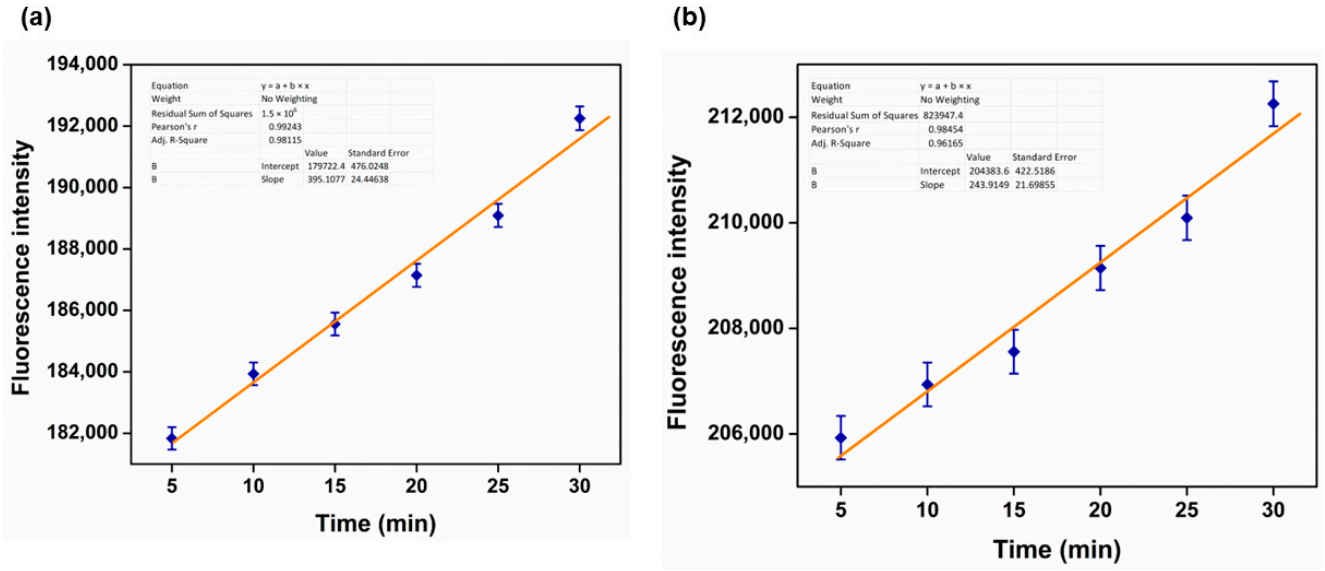

Figure 13. Linear graph of fluorescence intensity versus time of (**a**) Fe^{2+} and (**b**) Cu^{2+} at 390 nm upon excitation at 350 nm.

3.11. Logic Gate Construction

Molecular logic gates were designed for sensing applications using chemical sensors [29]. Based on the reversibility of **PMDP**'s detection of Cu^{2+} and Fe^{2+} ions by adding EDTA, a Boolean logic function was implemented. Use of **PMDP**'s output at an emission of 390 nm was made as a logic gate function. **PMDP** received multiple additions of Cu^{2+} ions and EDTA, Fe^{2+} ions, and EDTA (Figure 14). A strong fluorescence emission was treated as "ON" (output = 1), and a weak fluorescence emission was treated as "OFF" (output = 0). A significant reduction in fluorescence intensity was observed upon the addition of Cu^{2+}/Fe^{2+}

(input 1) to **PMDP**. With input 2, the **PMDP**'s fluorescence intensity was unaffected by the addition of EDTA alone. On the other hand, the addition of EDTA and Cu^{2+}/Fe^{2+} caused the **PMDP** to become fluorescent. When the outputs A and B were both "OFF", the fluorescence was also "OFF". With a NOT gate available for the Cu^{2+} and Fe^{2+} inputs, the logic function could be carried out. The OR gate function was utilised to represent the input–output combination of the **PMDP**-Cu^{2+}/Fe^{2+}-EDTA, as illustrated in Figure 14d.

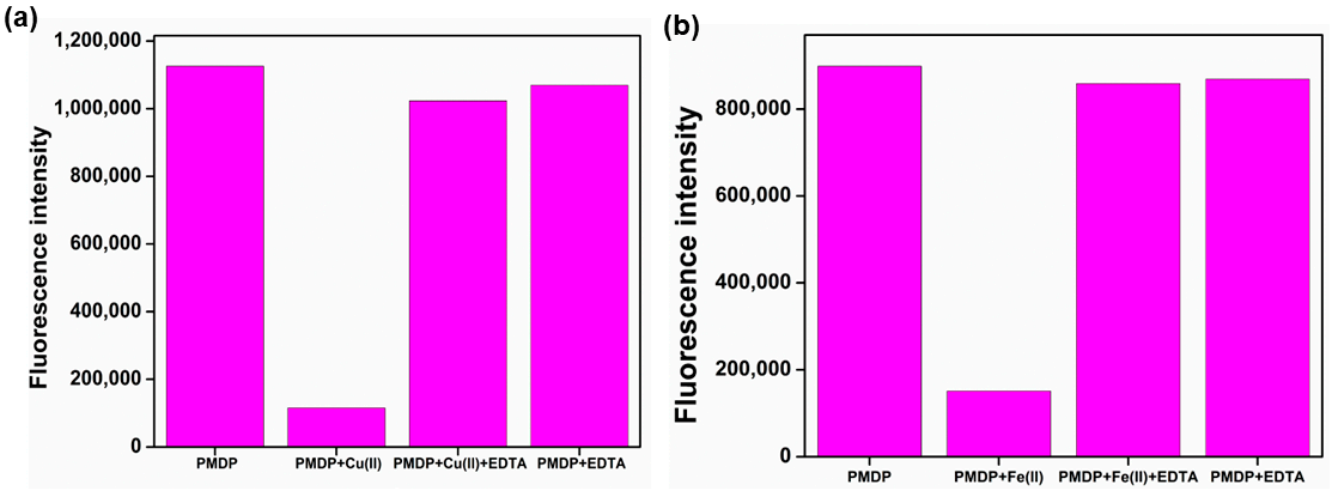

(c)

Input 1 (Cu^{2+} / Fe^{2+})	Output of Input 1 [A]	Input 2 (EDTA) [B]	Output of probe at 390 nm
0	1	0	1
1	0	0	0
1	0	1	1
0	1	1	1

(d)

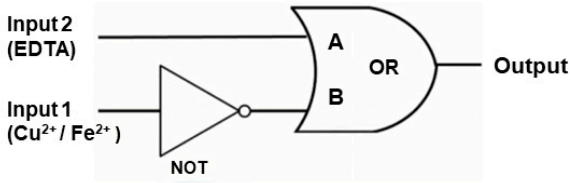

Figure 14. Change in fluorescence intensity at 390 nm upon excitation at 350 nm in the presence of four input combinations and (**a**) Cu^{2+} and (**b**) Fe^{2+} ions. (**c**) Truth table based on changes in emission intensity (390 nm) of **PMDP** by Cu^{2+} and Fe^{2+} and EDTA. (**d**) INHIBIT molecular logic gate of ligand **PMDP**.

3.12. Real Water Sample Analysis

To assess the potential usefulness of **PMDP** in tap and lake water samples, UV-Visible spectroscopy was used to broaden its practical applicability by utilising ambient water samples. Since the sensing metal must be identified using electronic absorption spectroscopy, real water samples were examined using a standard addition procedure [30,31]. Both tap water and lake water samples were taken from separate locations: Kukkralli Lake at the University of Mysore and a laboratory tap. In order to create spike samples, **PMDP** (30 mM) was added separately to different amounts of Cu^{2+} and Fe^{2+} ions (1 to 10 mM). Figure 15 shows that both the tap water and lake water exhibit a similar excitation peak at 300 nm, indicating that UV-Visible spectroscopy was used to examine **PMDP**'s sensing capability with the tested metal ions. The fact that **PMDP** can identify Cu^{2+} and Fe^{2+} in actual water samples is further supported by these findings.

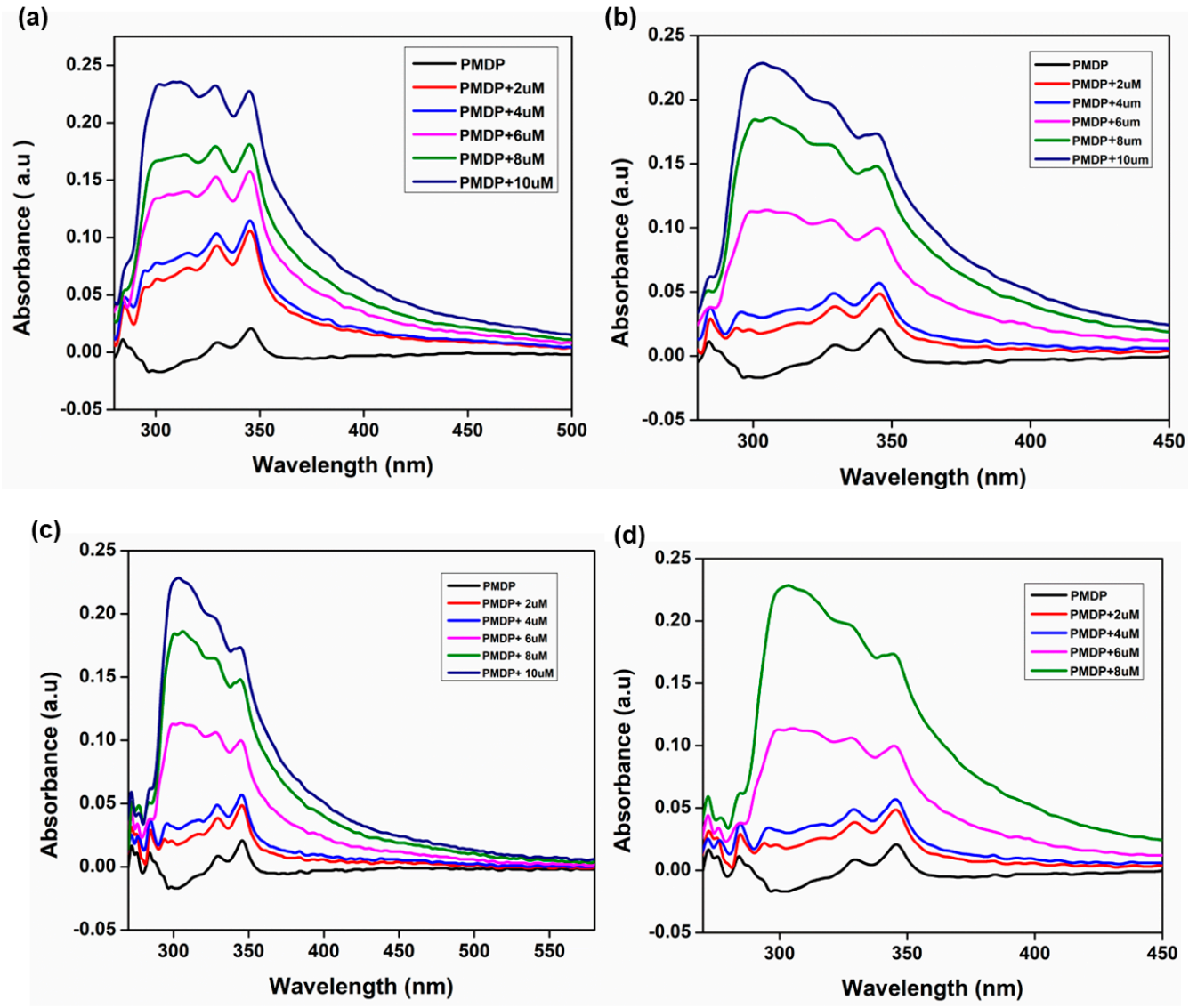

Figure 15. Absorbance spectra of real water sample analysis for detecting Fe^{2+} and Cu^{2+} ions: (**a**,**c**) lake water and (**b**,**d**) tap water.

3.13. Smartphone Application

Additionally, employing the free mobile app Colorimeter, which was downloaded to an iPhone 13, it was discovered that the R/G ratio increased in accordance with rising Cu^{2+} and Fe^{2+} concentration levels (Figure 16). To ensure that **PMDP** is operating as it should before and after the addition of different quantities of Cu^{2+} and Fe^{2+} (2–10.0 eq.), pictures were obtained using a camera. The relationship between the R/G ratio of the **PMDP** and the Cu^{2+} and Fe^{2+} is linear, as Figure 17 illustrates. For the Cu^{2+} and Fe^{2+} ions, the corresponding LOD values were found to be 0.42 µM and 0.51 µM. Thanks to smartphone applications, on-site Cu^{2+} and Fe^{2+} detection is now easy, quick, and reasonably priced [32,33].

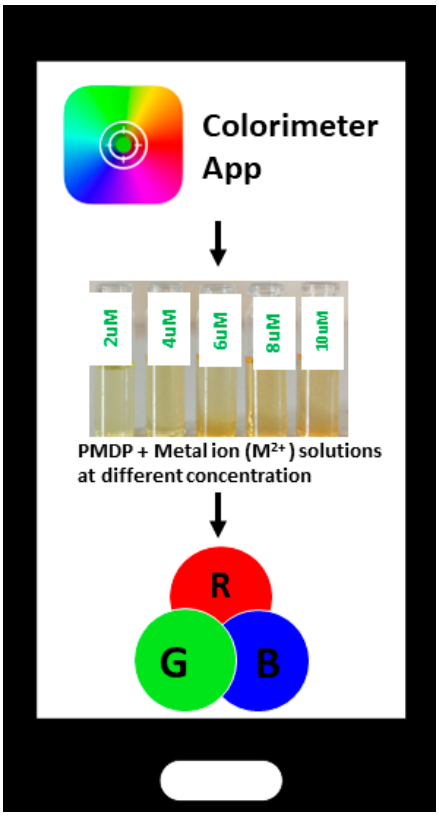

Figure 16. Schematic representation of the application of **PMDP** in smartphone-based RGB detection.

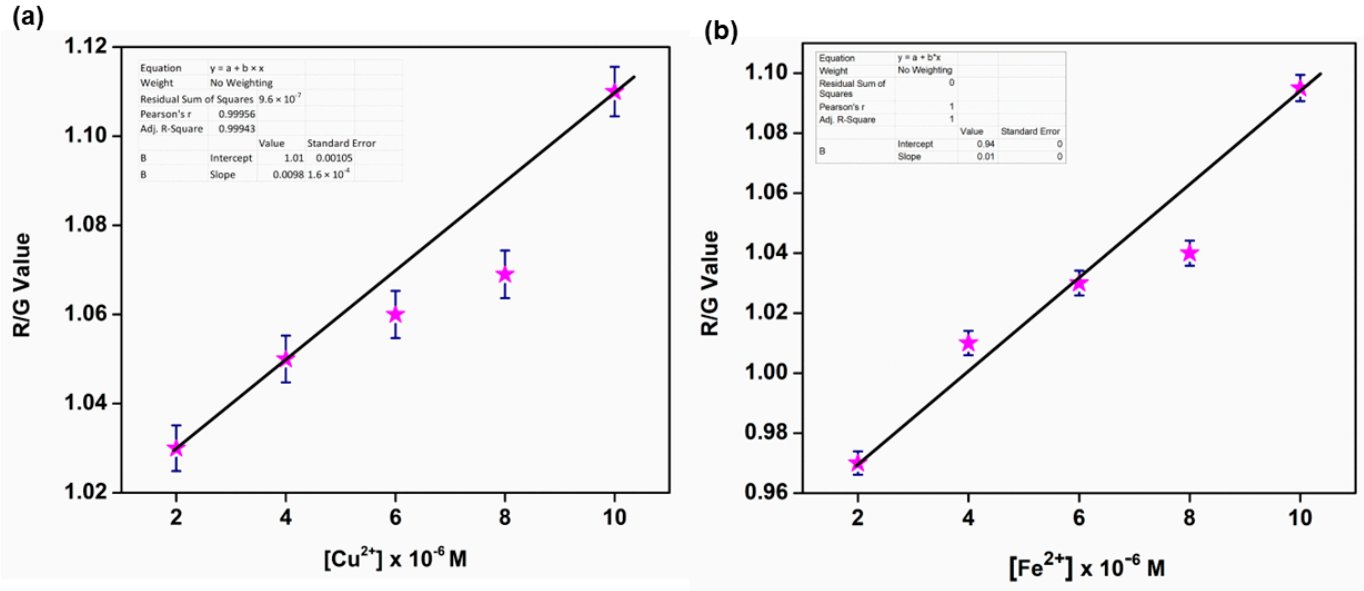

Figure 17. RGB-based calibration curve with smartphone assistance for (**a**) Cu^{2+} and (**b**) Fe^{2+} ions.

3.14. Sensing Mechanism

Considering the coordination model based on the experimental results (Figures S5 and S6), herein, we propose a mechanism of binding **PMDP** with Cu^{2+} and Fe^{2+} ions. The aforementioned metal ions attack the -NH part of the **PMDP** to deprotonate it and, in addition, to form a bond with the Schiff base N-atom (Figure 18). The excited-state intramolecular proton transfer (ESIPT) process explains the fluorescence quenching mechanism through the binding of deprotonated and Schiff base N-atoms with the Cu^{2+} and Fe^{2+} ions [34,35].

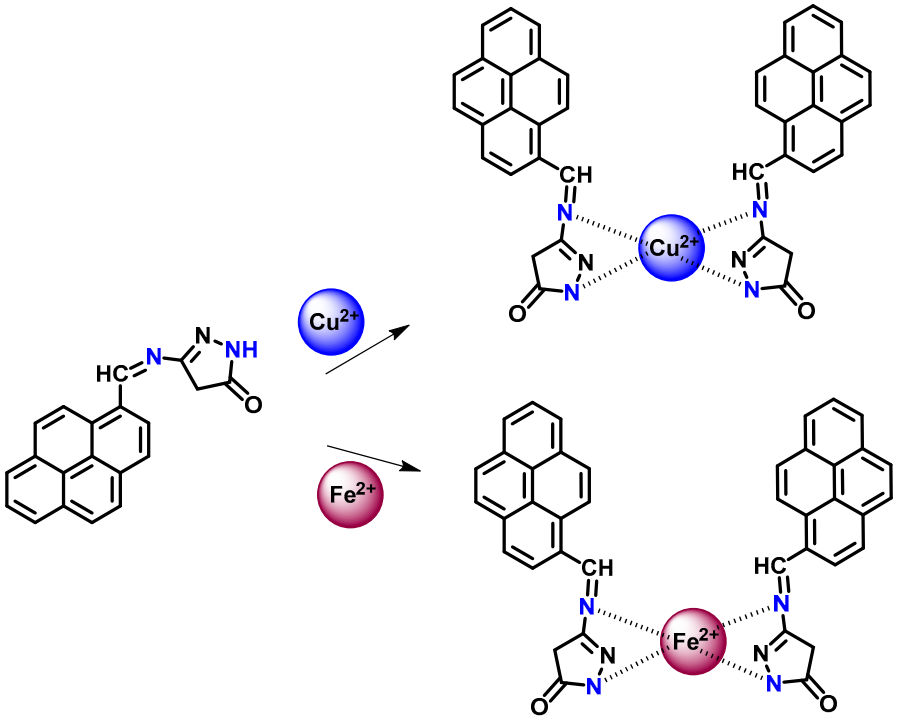

Figure 18. The proposed binding mechanism of the probe **PMDP** and Cu^{2+} and Fe^{2+} complexes.

3.15. Cytotoxicity and Cell Imaging Studies

An MTT assay was used to conduct cytotoxicity experiments on living HeLa cells at varying doses (0–20 μM) of **PMDP** and its Cu^{2+} and Fe^{2+} complexes. Figure 16 makes this very evident that the examined cells do not react toxically to the ligand or its complexes. To facilitate the fluorescence imaging of the cells, HeLa cells were cultivated with 30 μM **PMDP** and incubated for 30 min at 37 °C with 5% CO_2. Figure 19 demonstrates that the cell image did not exhibit fluorescence. After adding Cu^{2+} and Fe^{2+} ions (30 μM) and cultivating them as previously described, the sample was rinsed three times with PBS. Notably, the complex-containing cells are illuminated in green. Based on these findings, it can be said that the ligand **PMDP** is a suitable and biocompatible sensing probe for identifying Cu^{2+} and Fe^{2+} ions within live cells.

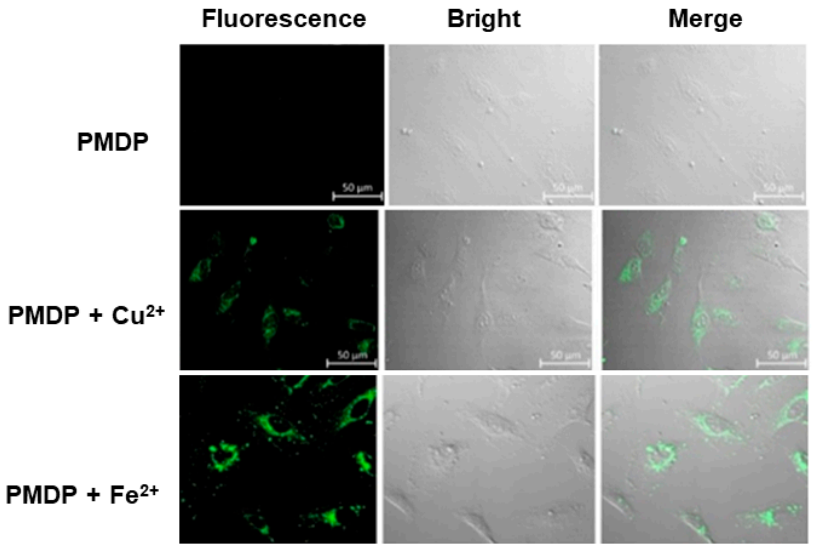

Figure 19. Bright-field and fluorescence images of HeLa cells following 30 min of incubation and treatment with 30 mol/L of **PMDP**, **PMDP** + Cu^{2+}, and **PMDP** + Fe^{2+}.

4. Conclusions

In summary, we effectively developed and synthesised a novel Schiff base as a chemical sensor (**PMDP**) based on pyrene-pyrazoles from 3-Amino-1H-pyrazol-5(4H)-one and 1-pyrenecarboxaldehyde. In a DMSO solution (HEPES, 10 mM pH 7.4) at room temperature, this allowed for the fluorescent, colorimetric detection of Cu^{2+} and Fe^{2+} ions with outstanding selectivity and sensitivity over other competitive ions. Using Job's plot, we found that **PMDP** has a 1:2 binding stoichiometry with Cu^{2+} and Fe^{2+} ions. The results revealed that the limits of detection for Cu^{2+} and Fe^{2+} are 0.42 μM and 0.51 μM, respectively. **PMDP** was discovered to be reversible towards the binding of Cu^{2+} and Fe^{2+} in the presence of EDTA; this technique was effectively applied in the building of a logic gate. Further, **PMDP** also demonstrated its operation in a wide pH range and was successfully applied to live cell imaging, a smartphone-based analysis, the creation of an INHIBIT-style logic gate, and the identification and quantification of Cu^{2+} and Fe^{2+} ions in environmental samples. In light of these results, we anticipate that the ligand **PMDP** will make a major contribution to the field of fundamental Schiff base sensors for the detection of Cu^{2+} and Fe^{2+} metal ions. The fact that **PMDP** demonstrated reversible binding and was non-toxic to cells is noteworthy.

Supplementary Materials: The following supporting information can be downloaded at https://www.mdpi.com/article/10.3390/chemosensors12060091/s1, Figure S1: ^{1}H NMR of **PMDP**, Figure S2: ^{13}C NMR of **PMDP**; Figure S3: MS of **PMDP**, Figure S4: MS of **PMDP**-Cu^{2+} complex and Figure S5: MS of **PMDP**-Fe^{2+} complex; Figure S6: FT-IR of **PMDP**.

Author Contributions: Conceptualization, B.G.G. and S.P.K.; methodology, B.G.G.; software, M.I.; validation, S.P.K. and M.I.; formal analysis, B.G.G.; investigation, B.G.G.; resources, S.P.K. and M.I.; data curation, B.G.G.; writing—original draft preparation, B.G.G. and M.I.; writing—review and editing, S.P.K.; visualization, S.P.K. and M.I.; supervision, S.P.K.; project administration, S.P.K.; funding acquisition, M.I. All authors have read and agreed to the published version of the manuscript.

Funding: The authors extend their appreciation to Researchers Supporting Project, number RSPD2024-R734, King Saud University, Riyadh, Saudi Arabia.

Data Availability Statement: The data are contained in the manuscript and the Supplementary Material.

Acknowledgments: The authors thankfully acknowledge the Amrita Vishwa Vidyapeetham, Mysuru Campus, for providing infrastructure facilities. The authors extend their appreciation to the Researchers Supporting Project, number RSPD2024R734, King Saud University, Riyadh, Saudi Arabia.

Conflicts of Interest: The authors declare no conflicts of interest.

References

1. Wei, T.-B.; Zhang, P.; Shi, B.-B.; Chen, P.; Lin, Q.; Liu, J.; Zhang, Y.-M. A highly selective chemosensor for colorimetric detection of Fe^{3+} and fluorescence turn-on response of Zn^{2+}. *Dye. Pigment.* **2013**, *97*, 297–302. [CrossRef]
2. Paul, B.K.; Kar, S.; Guchhait, N. A Schiff base-derived new model compound for selective fluorescence sensing of Cu(II) and Zn(II) with ratiometric sensing potential: Synthesis, photophysics and mechanism of sensory action. *J. Photochem. Photobiol. A Chem.* **2011**, *220*, 153–163. [CrossRef]
3. Jang, Y.K.; Nam, U.C.; Kwon, H.L.; Hwang, I.H.; Kim, C. A selective colorimetric and fluorescent chemosensor based-on naphthol for detection of Al^{3+} and Cu^{2+}. *Dye. Pigment.* **2013**, *99*, 6–13. [CrossRef]
4. Bravo, V.; Gil, S.; Costero, A.M.; Kneeteman, M.N.; Llaosa, U.; Mancini, P.M.E.; Ochando, L.E.; Parra, M. A new phenanthrene-based bis-oxime chemosensor for Fe(III) and Cr(III) discrimination. *Tetrahedron* **2012**, *68*, 4882–4887. [CrossRef]
5. Lukatkin, A.; Egorova, I.; Michailova, I.; Malec, P.; Strzałka, K. Effect of copper on pro- and antioxidative reactions in radish (*Raphanus sativus* L.) in vitro and in vivo. *J. Trace Elem. Med. Biol.* **2014**, *28*, 80–86. [CrossRef] [PubMed]
6. Pätsikkä, E.; Kairavuo, M.; Sersen, F.; Aro, E.-M.; Tyystjärvi, E. Excess Copper Predisposes Photosystem II to Photoinhibition in vivo by Outcompeting Iron and Causing Decrease in Leaf Chlorophyll. *Plant Physiol.* **2002**, *129*, 1359–1367. [CrossRef] [PubMed]
7. Hane, F.T.; Hayes, R.; Lee, B.Y.; Leonenko, Z. Effect of copper and zinc on the single molecule self-affinity of Alzheimer's amyloid-β peptides. *PLoS ONE* **2002**, *11*, e0147488. [CrossRef] [PubMed]
8. Lee, S.A.; Lee, J.J.; Shin, J.W.; Min, K.S.; Kim, C. A colorimetric chemosensor for the sequential detection of copper(II) and cysteine. *Dye. Pigment.* **2015**, *116*, 131–138. [CrossRef]

9. Shruthi, B.; Revanasiddappa, H.D.; Jayalakshmi, B.; Syed, A.; Elgorban, A.M.; Eswaramoorthy, R.; Amachawadi, R.G.; Shivamallu, C.; Kollur, S.P. Hydrobenzoic acid-based 'Turn-Off' fluorescent sensor for selective detection of Cu^{2+} ions: Chemical preparation, characterization and photophysical studies. *Inorg. Chem. Commun.* **2023**, *150*, 110467. [CrossRef]
10. Divyashree, N.R.; Revanasiddappa, H.D.; Bhavya, N.R.; Mahendra, M.; Jayalakshmi, B.; Shivamallu, C.; Prasad Kollur, S. Azaneylylidene-based tetradentate Schiff base as a new "ON-OFF" fluorescent probe for the detection of Cu(II) ion: Synthesis, characterization and real sample analysis. *Spectrochim. Acta Part A Mol. Biomol. Spectrosc.* **2023**, *292*, 122435. [CrossRef]
11. Bonda, D.J.; Lee, H.-G.; Blair, J.A.; Zhu, X.; Perry, G.; Smith, M.A. Role of metal dyshomeostasis in Alzheimer's disease. *Metallomics* **2011**, *3*, 267–270. [CrossRef]
12. Wang, L.; Yang, L.; Cao, D. A visual and fluorometric probe for Al(III) and Fe(III) using diketopyrrolopyrrole-based Schiff base. *Sens. Actuators B Chem.* **2014**, *202*, 949–958. [CrossRef]
13. Bansod, B.; Kumar, T.; Thakur, R.; Rana, S.; Singh, I. A review on various electrochemical techniques for heavy metal ions detection with different sensing platforms. *Biosens. Bioelectron.* **2017**, *94*, 443–455. [CrossRef] [PubMed]
14. Boulechfar, C.; Ferkous, H.; Delimi, A.; Djedouani, A.; Kahlouche, A.; Boublia, A.; Darwish, A.S.; Lemaoui, T.; Verma, R.; Benguerba, Y. Schiff bases and their metal Complexes: A review on the history, synthesis, and applications. *Inorg. Chem. Commun.* **2023**, *150*, 110451. [CrossRef]
15. Mohan, M.; James, J.; Satyanarayan, M.N.; Trivedi, D.R. Functionalized pyrene-based AIEgens: Synthesis, photophysical characterization and density functional theory studies. *Luminescence* **2019**, *34*, 715. [CrossRef] [PubMed]
16. Divyashree, N.R.; Revanasiddappa, H.D.; Yathirajan, H.S.; Bhavya, N.R.; Mahendra, M.; Muzaffar, I.; Chandan, S.; Raghavendra, G.A.; Shiva Prasad, K. Highly selective and sensitive fluorescent "TURN-ON" furan-based Schiff base for zinc(II) ion probing: Chemical synthesis, DFT studies, and X-ray crystal structure. *New J. Chem.* **2023**, *47*, 17420–17433. [CrossRef]
17. Liu, B.; Zhuang, J.; Wei, G. Recent advances in the design of colorimetric sensors for environmental monitoring. *Environ. Sci. Nano* **2020**, *7*, 2195–2213. [CrossRef]
18. Ayranci, R.; Karatas, E.; Ak, M. A new colorimetric sensor for Cu^{2+} detection based on s-triazine cored amino carbazole. *Mater. Res. Express* **2019**, *6*, 025504. [CrossRef]
19. Khairnar, N.; Tayade, K.; Sahoo, S.K.; Bondhopadhyay, B.; Basu, A.; Singh, J.; Singh, N.; Gite, V.; Kuwar, A. A highly selective fluorescent 'turn-on'chemosensor for Zn^{2+} based on a benzothiazole conjugate: Their applicability in live cell imaging and use of the resultant complex as a secondary sensor of CN−. *Dalton Trans.* **2015**, *44*, 2097–2102. [CrossRef]
20. Shylaja, A.; Roja, S.S.; Priya, R.V.; Kumar, R.R. Four-Component Domino Synthesis of Pyrazolo [3,4-h]quinoline-3-carbonitriles: "Turn-Off" Fluorescent Chemosensor for Fe^{3+} Ions. *J. Org. Chem.* **2018**, *83*, 14084–14090. [CrossRef]
21. Panchal, U.; Modi, K.; Dey, S.; Prajapati, U.; Patel, C.; Jain, V.K. A resorcinarene-based "turn-off" fluorescence sensor for 4-nitrotoluene: Insights from fluorescence and ^1H NMR titration with computational approach. *J. Lumin.* **2017**, *184*, 74–82. [CrossRef]
22. Bhalla, V.; Sharma, N.; Kumar, N.; Kumar, M. Rhodamine based fluorescence turn-on chemosensor for nanomolar detection of Fe^{3+} ions. *Sens. Actuators B Chem.* **2013**, *178*, 228–232. [CrossRef]
23. Kumar, N.; Jung, U.; Jung, B.; Park, J.; Naushad, M. Zinc hydroxystannate/zinc-tin oxide heterojunctions for the UVC-assisted photocatalytic degradation of methyl orange and tetracycline. *Environ. Pollut.* **2023**, *316*, 120353. [CrossRef]
24. Barmatov, E.; Hughes, T. Degradation of a schiff-base corrosion inhibitor by hydrolysis, and its effects on the inhibition efficiency for steel in hydrochloric acid. *Mater. Chem. Phys.* **2021**, *257*, 123758. [CrossRef]
25. Yan, S.; Li, Y.; Yang, X.; Jia, X.; Xu, J.; Song, H. Photocatalytic H2O2 Generation Reaction with a Benchmark Rate at Air-Liquid-Solid Joint Interfaces. *Adv. Mater.* **2024**, *36*, 2307967. [CrossRef] [PubMed]
26. Kumar, R.; Ravi, S.; Immanuel David, C.; Nandhakumar, R. A photo-induced electron transfer based reversible fluorescent chemosensor for specific detection of mercury (II) ions and its applications in logic gate, keypad lock and real samples. *Arab. J. Chem.* **2021**, *14*, 102911. [CrossRef]
27. Kim, A.; Kim, S.; Kim, C. A conjugated Schiff base-based chemosensor for selectively detecting mercury ion. *J. Chem. Sci.* **2020**, *132*, 82. [CrossRef]
28. Gupta, N.; Singhal, D.; Singh, A.K. Highly selective colorimetric and reversible fluorometric turn-off sensors based on the pyrimidine derivative: Mimicking logic gate operation and potential applications. *New J. Chem.* **2016**, *40*, 641–650. [CrossRef]
29. Sharma, S.; Chayawan; Debnath, J.; Sundar Ghosh, K. Method for highly selective, ultrasensitive fluorimetric detection of Cu^{2+} and Al^{3+} by Schiff bases containing o-phenylenediamine and o-aminophenol. *Methods* **2023**, *217*, 27–35. [CrossRef]
30. Sahoo, S.K.; Crisponi, G. Recent Advances on Iron(III) Selective Fluorescent Probes with Possible Applications in Bioimaging. *Molecules* **2019**, *24*, 3267. [CrossRef]
31. Divyashree, N.R.; Revanasiddappa, H.D.; Jayalakshmi, B.; Iqbal, M.; Amachawadi, R.G.; Shivamallu, C.; Prasad Kollur, S. 'Turn-ON' furfurylamine-based fluorescent sensor for Cd^{2+} ion detection and its application in real water samples. *Polyhedron* **2023**, *238*, 116411. [CrossRef]
32. Kathirvel, R.; Poongodi, M.; Vetriarasu, V.; Vivekanandan, K.E.; Selvakumar, K.; Al Obaid, S.; Pugazhendhi, A.; Venkatesan, G. Quinoline-quinoline Schiff-base as an effective chromogenic, fluorogenic, and smartphone assisted RGB detection of Pb^{2+} ion in near aqueous medium. *Environ. Res.* **2024**, *250*, 118530. [CrossRef]

33. Manna, A.K.; Sahu, M.; Rout, K.; Das, U.K.; Patra, G.K. A highly selective novel multiple amide-based Schiff base optical chemosensor for rapid detection of Cu^{2+} and its applications in real sample analysis, molecular logic gate and smart phone. *Microchem. J.* **2020**, *157*, 104860. [CrossRef]
34. Liu, S.; Wang, Y.-M.; Han, J. Fluorescent chemosensors for copper(II) ion: Structure, mechanism and application. *J. Photochem. Photobiol. C Photochem. Rev.* **2017**, *32*, 78. [CrossRef]
35. Rasin, P.; Mathew, M.M.; Manakkadan, V.; Palakkeezhillam, V.N.V.; Sreekanth, A. A Highly Fluorescent Pyrene-Based Sensor for Selective Detection Of Fe^{3+} Ion in Aqueous Medium: Computational Investigations. *J. Fluoresc.* **2022**, *32*, 1229. [CrossRef]